Archives of Materials Science and Engineering

Volume 64
Issue 2
December 2013
Pages 97-102

International Scientific Journal published monthly by the World Academy of Materials and Manufacturing Engineering

Structure and magnetic properties of bulk amorphous $(Fe_{0.61}Co_{0.10}Zr_{0.025}Hf_{0.025}W_{0.02}Ti_{0.02}B_{0.20})_{94}Y_6$ alloy

K. Błoch*

Institute of Physics, Faculty of Materials Processing Technology and Applied Physics, Czestochowa University of Technology, Al. Armii Krajowej 19, 42-200 Częstochowa, Poland

* Corresponding e-mail address: 23kasia1@wp.pl

Received 17.10.2013; published in revised form 01.12.2013

ABSTRACT

Purpose: The aim of this paper were studies of the structure and magnetic properties of the bulk amorphous $(Fe_{0.61}Co_{0.10}Zr_{0.025}Hf_{0.025}W_{0.02}Ti_{0.02}B_{0.20})_{94}Y_6$ alloy, obtained by suction-casting method.

Design/methodology/approach: The microstructure of the as-quenched and annealed at 720K for 15 min samples was studied by X-ray diffractometry and Mössbauer spectroscopy. The transmission Mössbauer spectra for the powdered samples were measured at room temperature using conventional Mössbauer spectrometer working at a constant acceleration with a $^{57}Co(Rh)$ radioactive source of the 70 mCi in activity. However, the low field magnetic properties such as magnetic susceptibility, its disaccommodation and core losses were measured by a transformer method using a completely automated set up. In susceptibiity and its disaccommodation studies the amplitude of the magnetizing field was 0.26 A/m. Before the measurements the samples were demagnetized in an alternating magnetic field with the amplitude decreasing from 800 A/m to zero during 1.1 s. The core losses and magnetic permeability as a function of the magnetizing field amplitude for the frequency up to 1 kHz were measured.

Findings: The rods were fully amorphous which was confirmed by X-ray diffractometry and Mössbauer spectroscopy. On the basis studies of magnetization in high magnetic fields we have stated, that in investigated alloy, in the as-quenched state and after annealing, only structural defects called quasi-dislocation dipoles are present. The disaccommodation phenomenon in the investigated samples of $(Fe_{0.61}Co_{0.10}Zr_{0.025}Hf_{0.025}W_{0.02}Ti_{0.02}B_{0.20})_{94}Y_6$ alloy , related with the directional ordering of atomic pairs near the free volumes, is not observed. On the basis of the changes in core losses, it can be stated that the studied alloy at low frequencies the total losses are comparable with those observed in classical silicon-iron alloys.

Practical implications: Using a vibrating sample magnetometer the magnetization in high magnetic fields was studied (in magnetic field up to 2 T). All investigations carried out for samples in the as-quenched state and after annealing.

Originality/value: This paper presents studies relating to the structure and magnetic properties of the bulk amorphous $(Fe_{0.61}Co_{0.10}Zr_{0.025}Hf_{0.025}W_{0.02}Ti_{0.02}B_{0.20})$ alloy, obtained in the form of rods with 2 mm in diameter and 2 cm long by the suction casting method.

Keywords: Bulk amorphous alloy; Microstructure; Permeability and it's disaccommodation; Approach to saturation magnetization; Core losses

Reference to this paper should be given in the following way:

K. Błoch, Structure and magnetic properties of bulk amorphous $(Fe_{0.61}Co_{0.10}Zr_{0.025}Hf_{0.025}W_{0.02}Ti_{0.02}B_{0.20})_{94}Y_6$ alloy, Archives of Materials Science and Engineering 64/2 (2013) 97-102.

MATERIALS

1. Introduction

The bulk amorphous materials are usually multicomponent systems and consist of more than three elements. They are obtained by a rapid solidification of liquid materials in a copper mold cooled with water [1-3]. In order to obtain an amorphous structure in these alloys two additional rules must be fulfilled: the difference in the atomic radii of main components should be larger than 12% and he main elements should exhibit negative heat of mixing, which leads to the increase of the viscosity of the molten alloy [4, 5]. It is worth noticing that the bulk amorphous alloys are prepared with lower quenching rate than classical ones. Due to relatively low quenching rate the bulk amorphous alloys after solidification are partially relaxed and they exhibit good time and thermal stability of the structure and magnetic properties [6,7].

In this paper we present results of the structure and magnetic properties studies of the bulk amorphous $(Fe_{0.61}Co_{0.10}Zr_{0.025}Hf_{0.025}W_{0.02}Ti_{0.02}B_{0.20})_{94}Y_6$ alloy in the form of rods.

2. Materials and methodology

Ingots of the alloys were prepared by arc melting of high purity elements in an argon atmosphere. The samples of the $(Fe_{0.61}Co_{0.10}Zr_{0.025}Hf_{0.025}W_{0.02}Ti_{0.02}B_{0.20})_{94}Y_6$ alloy were obtained in the form of rods 2 mm in diameter and 2 cm long by the suction casting method. The microstructure of the as-quenched and annealed at 720K for 15min samples was studied by X-ray diffractometry and Mössbauer spectroscopy. The transmission Mössbauer spectra for the powdered samples were measured at room temperature using conventional Mössbauer spectrometer working at a constant acceleration with a ^{57}Co(Rh) radioactive source of the 70 mCi in activity. The spectra were fitted by Normos package [8]. However, the low field magnetic properties such as magnetic susceptibility and its disaccommodation were measured by a transformer method using a completely automated set up. Measurements of the magnetic susceptibility χ were performed with a magnetizing field of amplitude 0.26 A/m. A Ferrometer was used for the determination of core losses. Additionally, using a vibrating sample magnetometer the magnetization in high magnetic fields was studied (in magnetic field up to 2 T).

3. Results and discussion

In Fig. 1 X-ray diffraction patterns for the powdered bulk $(Fe_{0.61}Co_{0.10}Zr_{0.025}Hf_{0.025}W_{0.02}Ti_{0.02}B_{0.20})_{94}Y_6$ alloy in the as-quenched state and after annealing at 720 K for 15 min are shown. As can be seen, the diffraction patterns exhibit only broad single maxima which are typical of amorphous materials. No sharp peaks ascribed to the crystalline phase are visible, so the samples are fully amorphous.

The transmission Mössbauer spectra and corresponding hyperfine field induction distributions for tested alloy in the as-quenched state and after annealing at 720 K for 15 min are presented in Fig. 2.

The Mössbauer spectrum consists of broad and overlapped lines which is characteristic of the amorphous state. The average induction of the hyperfine field at ^{57}Fe nuclei (B_{eff}) in these samples in the as-quenched state is equal to 12.90 T. The hyperfine field distribution obtained from the Mössbauer spectrum is asymmetric and at least three components can be distinguished. It indicates that the investigated alloy is not homogeneous and consists of regions with different iron concentration. It is worth adding that after the annealing of the rod at 720K for 15min Mössbauer spectrum is almost the same. The average induction of the hyperfine field (B_{eff}) for investigated alloy after annealing is equal to 12.05 T.

The Mössbauer spectroscopy can distinguish atomically, magnetically or electronically in-equivalent lattice sites. Moreover, these studies provide information about local neighborhood in clearly defined area. On the basis of Mössbauer spectroscopy studies it was found that in the tested alloy after isothermal annealing process, there has been a redistribution its chemical components, as demonstrated by changes in the first wing of the hyperfine field distribution (B_{hf} is equal to 3T). The hyperfine field distribution B_{hf} for the other two maxima was practically the same. The low-field wing in B_{hf} distribution is associated with the iron atoms, which have atoms Y in their the nearest environment. It is known, that transition metals such as Cu and Nb in the first coordination shell of iron causes a decrease B_{hf} values for iron atoms [9,10]. The changes in the probability $P(B_{hf})$ for sample after annealing relative to the material in the state after solidification are caused by the modification of the distribution B_{hf}. It should be noted, that these studies give an opportunity to observe only the nearest environment of the Fe atoms and therefore it is possible to use this information when the Y atoms migrate from areas rich in Fe, after annealing process.

This behavior is related to the relaxation processes taking place in the amorphous materials at the elementary level. The spatial distribution of alloy components due to fluctuations in the composition leads to the diffusion of Y atoms from the zones rich in Fe.

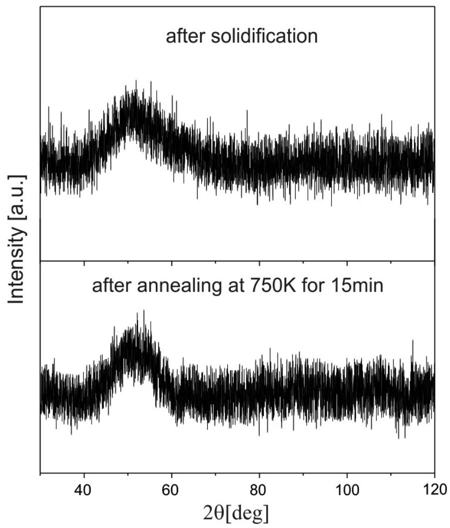

Fig. 1. X-ray diffraction patterns for $(Fe_{0.61}Co_{0.10}Zr_{0.025}Hf_{0.025}W_{0.02}Ti_{0.02}B_{0.20})_{94}Y_6$ alloy in the as-quenched state (a) and after annealing at 720 K for 15 min (b)

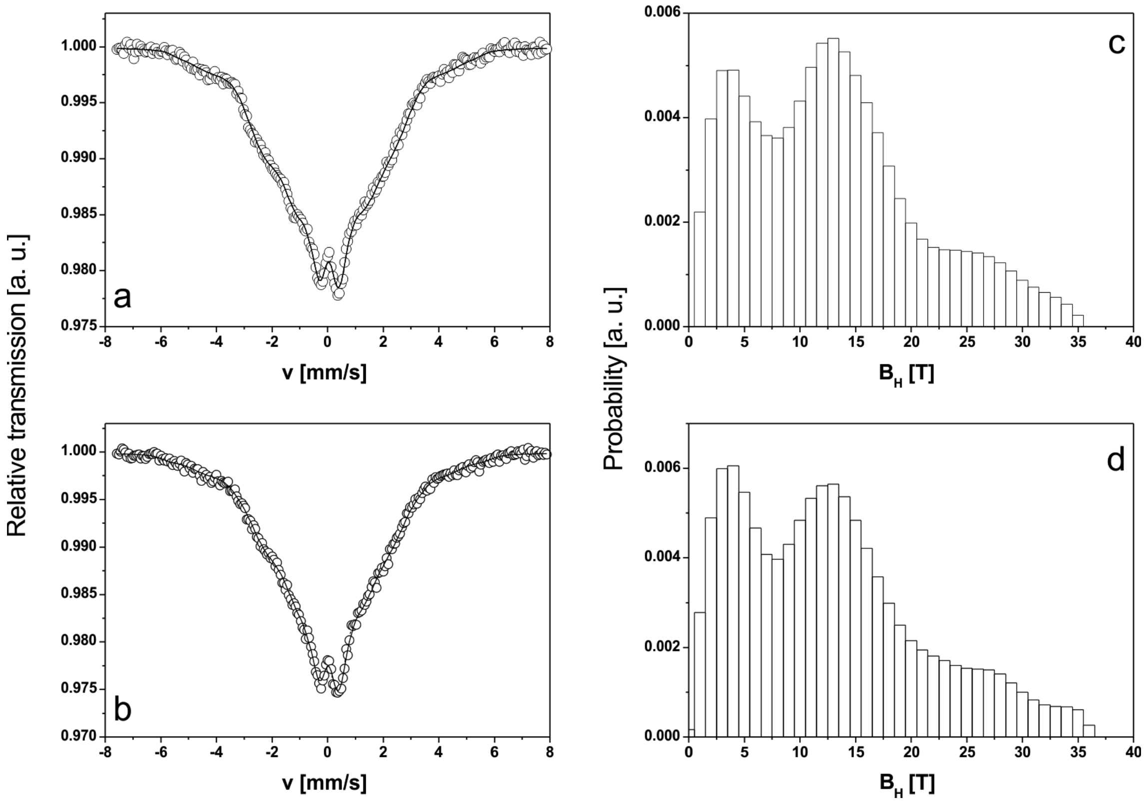

Fig. 2. Mössbauer spectra (a, b) and corresponding hyperfine field induction distributions (c, d) for $(Fe_{0.61}Co_{0.10}Zr_{0.025}Hf_{0.025}W_{0.02}Ti_{0.02}B_{0.20})_{94}Y_6$ alloy in the as-quenched state (a, c) and after annealing at 720K for 15min (b, d)

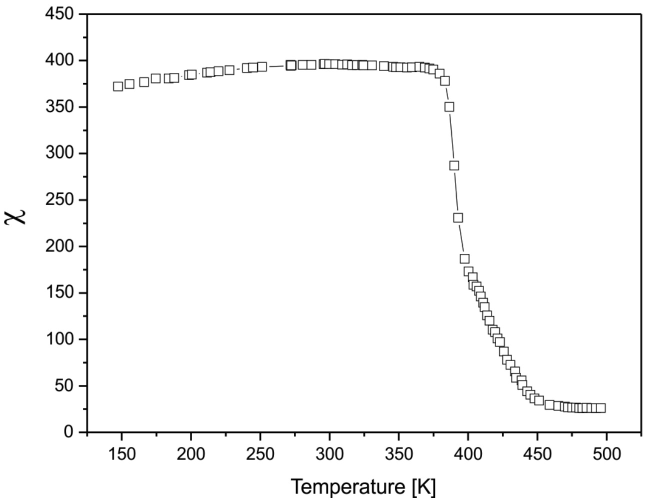

Fig. 3. Low field magnetic susceptibility versus temperature for $(Fe_{0.61}Co_{0.10}Zr_{0.025}Hf_{0.025}W_{0.02}Ti_{0.02}B_{0.20})_{94}Y_6$ alloy in the as-quenched state

In Figs. 3, 4 low field magnetic susceptibility of the alloys versus temperature is depicted. The studies of the magnetic susceptibility were performed in the low magnetic field range of $<H<0.4H_c$. In this range, only reversible magnetic processes are taking place.

The initial magnetic susceptibility of the alloy in the as-quenched state and after annealing is almost constant up to Curie temperature, i.e. 375 K. Such behavior indicates a very good thermal stability of the magnetic properties of investigated alloy. For higher temperatures ($>T_c$) magnetic susceptibility χ drastically decreases. It is related to the phase transition from a ferromagnetic to a paramagnetic state.

On the basis of studies of the magnetic susceptibility as a function of time the disaccommodation of the magnetic susceptibility has been calculated.

Figures 5, 6 show the isochronal magnetic susceptibility disaccommodation curves $\Delta(1/\chi)=f(T)$ obtained for the tested alloy after solidification and annealing state.

The $(Fe_{0.61}Co_{0.10}Zr_{0.025}Hf_{0.025}W_{0.02}Ti_{0.02}B_{0.20})_{94}Y_6$ alloy shows also very low intensity of the magnetic susceptibility disaccommodation and in isochronal disaccommodation curves only temperature independent background is observed. The disaccommodation phenomenon in the amorphous alloys is related with the directional ordering of atomic pairs near the free volumes. On the basis studies of magnetization in high magnetic fields we have stated, that in investigated alloy in the as-quenched state and after annealing, only structural defects called quasi-dislocation dipoles are present. Magnetization of the bulk amorphous $(Fe_{0.61}Co_{0.10}Zr_{0.025}Hf_{0.025}W_{0.02}Ti_{0.02}B_{0.20})_{94}Y_6$ alloy in high magnetic fields may be described by the equation [11-12]:

$$\mu_0 M(H) = \mu_0 M_s \left[1 - \frac{a_1}{(\mu_0 H)^1} - \frac{a_2}{(\mu_0 H)^2} \right] + b(\mu_0 H)^{1/2}, \qquad (1)$$

where:
μ_0 - vacuum permeability,
Ms - saturation magnetization,
H - magnetic field,
a_i and b - coefficients,
i = 1 or 2.

The last element is associated with damping of thermally excited spin waves by a magnetic field - Holstein-Primakoff paraprocess [13].

In Figs. 7-9, high field magnetization curves for the investigated sample are shown.

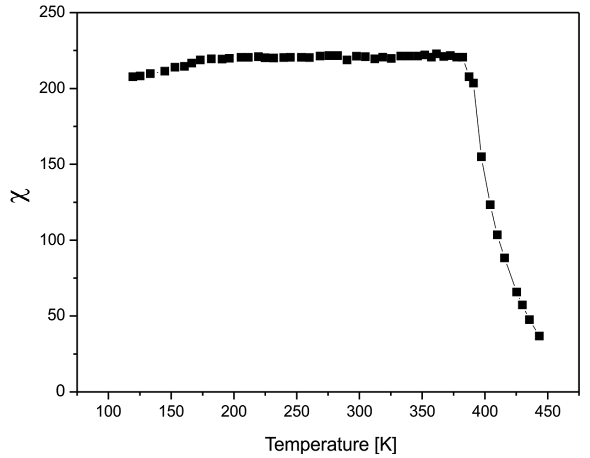

Fig. 4. Low field magnetic susceptibility versus temperature for $(Fe_{0.61}Co_{0.10}Zr_{0.025}Hf_{0.025}W_{0.02}Ti_{0.02}B_{0.20})_{94}Y_6$ alloy after annealing at 720 K for 15 min

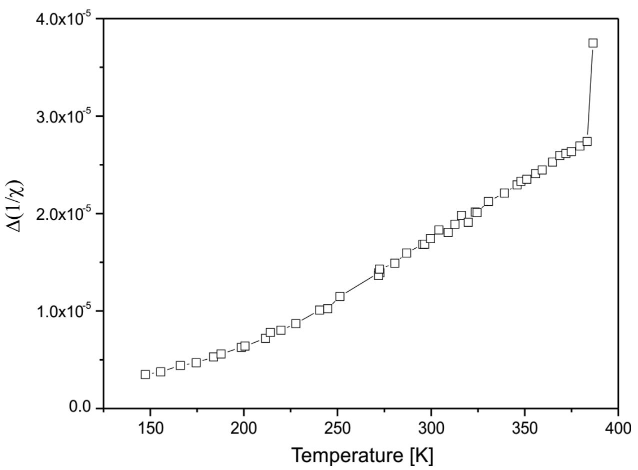

Fig. 5. The isochronal magnetic susceptibility disaccommodation curve Δ(1/χ)=f(T) for the $(Fe_{0.61}Co_{0.10}Zr_{0.025}Hf_{0.025}W_{0.02}Ti_{0.02}B_{0.20})_{94}Y_6$ after solidification

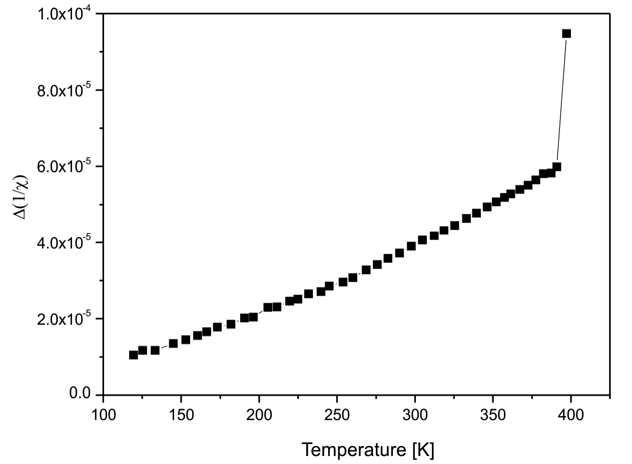

Fig. 6. The isochronal magnetic susceptibility disaccommodation curve Δ(1/χ)=f(T) for the $(Fe_{0.61}Co_{0.10}Zr_{0.025}Hf_{0.025}W_{0.02}Ti_{0.02}B_{0.20})_{94}Y_6$ alloy after annealing at 720 K for 15 min

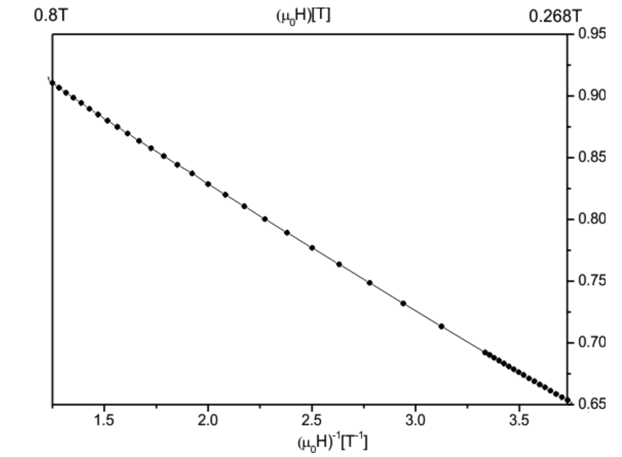

Fig. 7. The high field magnetization curves $M/M_S((\mu_0H)^{-1})$ for the $(Fe_{0.61}Co_{0.10}Zr_{0.025}Hf_{0.025}W_{0.02}Ti_{0.02}B_{0.20})_{94}Y_6$ alloy after solidification

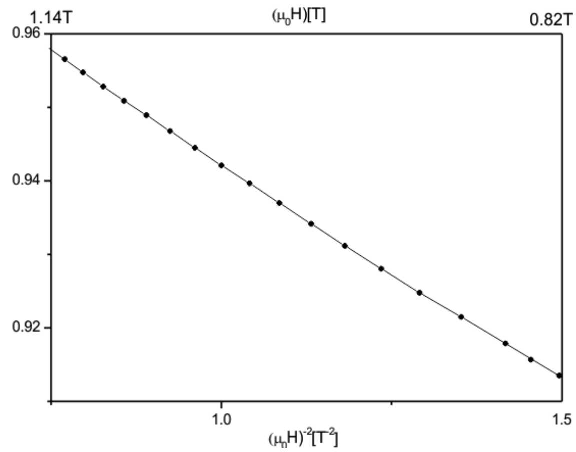

Fig. 8. The high field magnetization curves $M/M_S((\mu_0H)^{-2})$ for the $(Fe_{0.61}Co_{0.10}Zr_{0.025}Hf_{0.025}W_{0.02}Ti_{0.02}B_{0.20})_{94}Y_6$ alloy after solidification

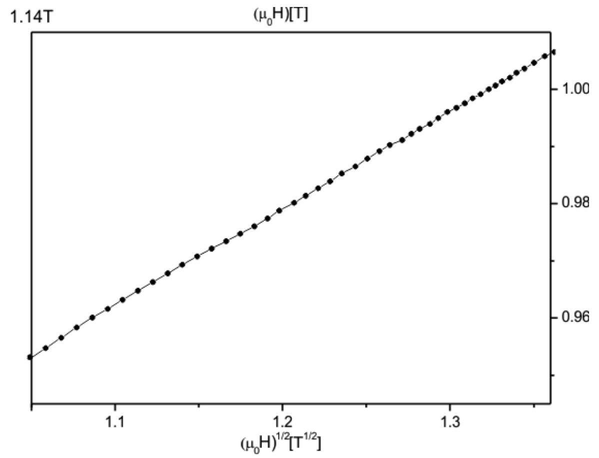

Fig. 9. The high field magnetization curves $M/M_S((\mu_0 H)^{1/2})$ for the investigated alloy, after solidification

In the range magnetic fields from 0.27 T to 0.8 T, the magnetization fulfils $M/M_S \sim 1/\mu_0 H$ law, pointing out the presence of quasi-dislocation dipoles with the width lower than the exchange length. The linear dependence of $M/M_S((\mu_0 H)^{-2})$ in magnetic field range from 0.8 T to 1.14 T is observed. Such behavior proves that in this magnetizing field range the magnetization process takes place by microscopic rotations of magnetic moments near quasi-dislocation dipoles for which the dependence $l_H^{-1} D_{dip} > 1$ (where: (l_H) - the reciprocal of the exchange length and (D_{dip}) -dipole width) is fulfilled. However, in magnetizing field induction higher than 1.14 T the Holstein-Primakoff process occurs (Fig. 9). For the alloy after heat treatment the same dependences were observed.

In a magnetic field ($>0.4H_C$), during the magnetisation process of the alloy, irreversible processes take place, and magnetic hysteresis is observed. The area of the hysteresis loop is a measure of the total core losses.

In Figs. 10, 11 the total core losses of the $(Fe_{0.61}Co_{0.10}Zr_{0.025}Hf_{0.025}W_{0.02}Ti_{0.02}B_{0.20})_{94}Y_6$ alloy are shown.

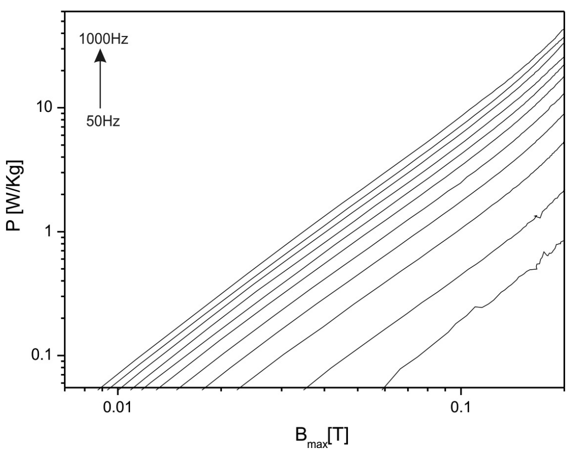

Fig. 10. The total core losses of the investigated alloy in the as-quenched state

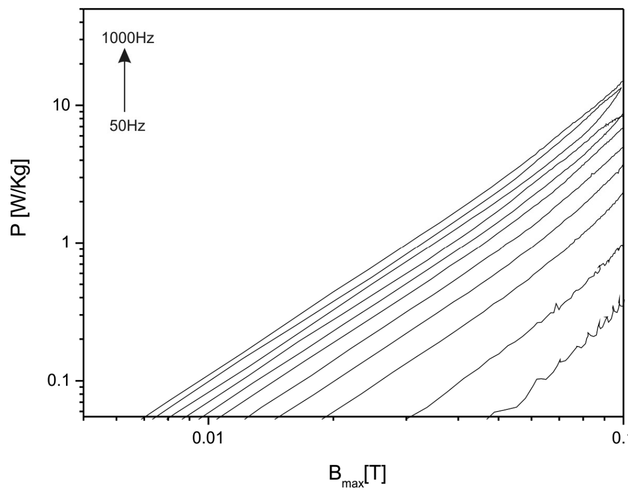

Fig. 11. The total core losses of the $(Fe_{0.61}Co_{0.10}Zr_{0.025}Hf_{0.025}W_{0.02}Ti_{0.02}B_{0.20})_{94}Y_6$ after annealing at 720 K for 15 min

The core losses of the bulk amorphous $(Fe_{0.61}Co_{0.10}Zr_{0.025}Hf_{0.025}W_{0.02}Ti_{0.02}B_{0.20})_{94}Y_6$ alloy are comparable with those for classical crystalline soft magnetic materials.

The magnetic permeability versus the amplitude of magnetizing field, measured at different frequencies for the investigated alloy is shown in Figs. 12, 13.

The maxima on the curve of magnetic permeability for the $(Fe_{0.61}Co_{0.10}Zr_{0.025}Hf_{0.025}W_{0.02}Ti_{0.02}B_{0.20})_{94}Y_6$ alloy- in the as-qunched state and after annealing at the frequency of 50Hz are equal 1050 and 580, respectively.

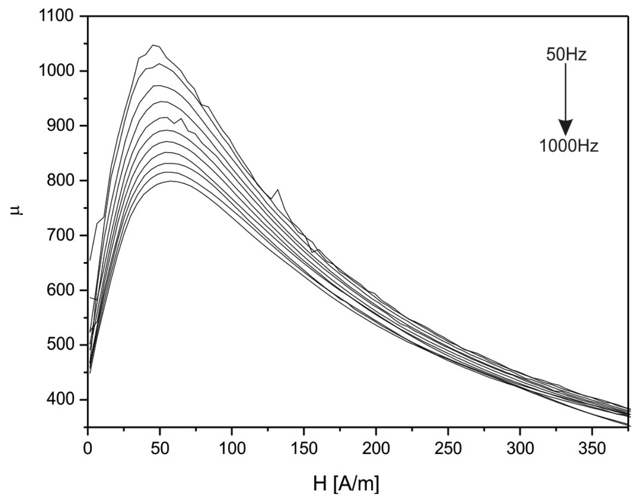

Fig. 12. Magnetic permeability versus the amplitude of magnetizing field as a function of the magnetizing field amplitude for the frequency up to 1 kHz for the bulk amorphous $(Fe_{0.61}Co_{0.10}Zr_{0.025}Hf_{0.025}W_{0.02}Ti_{0.02}B_{0.20})_{94}Y_6$ alloy in the as-quenched state

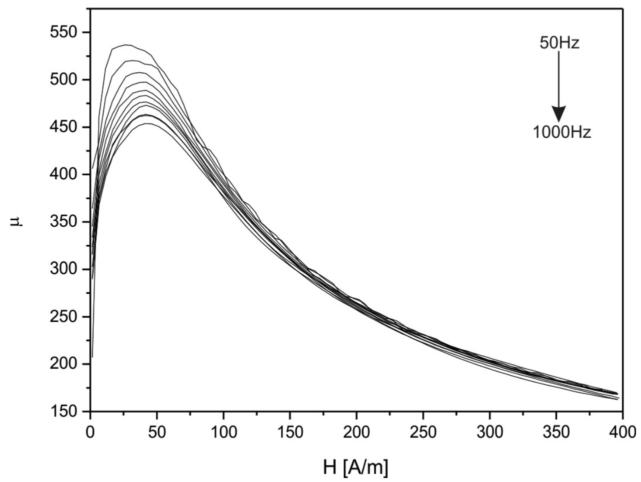

Fig. 13. Magnetic permeability versus the amplitude of magnetizing field as a function of the magnetizing field amplitude for the frequency up to 1 kHz for the investigated alloy after annealing at 720 K for 15 min

Figure 14 presents total core losses (P) versus square of the magnetizing field frequency for the amorphous $(Fe_{0.61}Co_{0.10}Zr_{0.025}Hf_{0.025}W_{0.02}Ti_{0.02}B_{0.20})_{94}Y_6$ material.

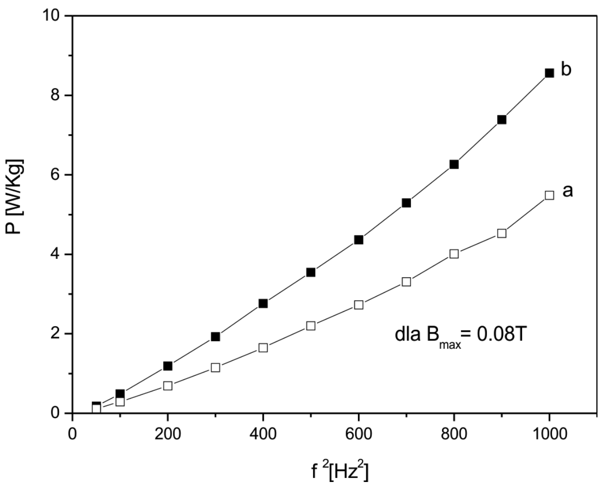

Fig. 14. The total core losses (P) versus square of the magnetizing field frequency for the bulk amorphous $(Fe_{0.61}Co_{0.10}Zr_{0.025}Hf_{0.025}W_{0.02}Ti_{0.02}B_{0.20})_{94}Y_6$ alloy in the as-quenched state (a) and after annealing at 720 K for 15 min (b)

As you can see from Fig. 10, linear dependence $P(f^2)$ is not observed. This behavior indicates the significant contribution of hysteresis and eddy current losses.

4. Conclusions

From the obtained results the following conclusions can be drawn. On the basis the X-ray diffractometry and Mössbauer spectroscopy studies we can stated, that investigated alloy in the as-quenched state and after annealing was fully amorphous Approach to magnetic saturation for the bulk amorphous $(Fe_{0.61}Co_{0.10}Zr_{0.025}Hf_{0.025}W_{0.02}Ti_{0.02}B_{0.20})_{94}Y_6$ alloy is achieved by the microscopic rotations of magnetic moments near the quasi-dislocation dipoles for which the dependences $l_H^{-1}D_{dip}<1$ and $l_H^{-1}D_{dip}>1$ are fullfilled The disaccommodation phenomenon in the investigated samples, related with the directional ordering of atomic pairs near the free volumes, is not observed. On the basis of the changes in core losses, it can be stated that the studied alloy at low frequencies the total losses are comparable with those observed in classical silicon-iron alloys.

References

[1] A. Inoue: Bulk Amorphous Alloys-Preparation and Fundamental Characteristics-, Materials Science Foundations 4, Trans Tech Publications, Netherlands (1998) 1-116.

[2] J. Zbroszczyk, J. Olszewski, W. Ciurzyńska, M. Nabiałek, P. Pawlik, M. Hasiak, A. Łukiewska, K. Perduta, Glass-forming ability and magnetic properties of bulk $Fe_{61}Co_{10}Zr_{2.5}Hf_{2.5}W_{4-y}Me_yB_{20}$ (y=0 or 2, Me=Mo, Nb, Ti) alloys., Journal of Magnetism and Magnetic Materials, 304/2 (2006) 724-726.

[3] A. Inoue, Bulk amorphous alloys with soft and hard magnetic properties, Materials Science and Engineering A226-228 (1997) 357-363.

[4] A. Inoue, A. Makino, T. Mizushima, Ferromagnetic bulk glassy alloys, Journal of Magnetism and Magnetic Materials 246 (2000) 215-216.

[5] A. Inoue, W. Zhang, T. Zhang, K. Kurosaka High-strength Cu-based bulk glassy alloys in Cu-Zr-Ti and Cu-Hf-Ti ternary systems Acta materalia 49 (2001) 2645-2652.

[6] M. Hasiak, K. Sobczyk, J. Zbroszczyk, W. Ciurzyńska, J. Olszewski, M. Nabiałek, J. Kaleta, J. Świerczek, A. Łukiewska, Some magnetic properties of bulk amorphous $(Fe_{61}Co_{10}Zr_{2.5}Hf_{2.5}Ti_2W_2B_{20})_{100-x}Y_x$ (x = 0 or 2) alloy IEEE Transactions on Magnetics 11 (2008) 3879.

[7] K. Sobczyk, J. Świerczek, J. Gondro, J. Zbroszczyk, W. Ciurzyńska, J. Olszewski, P. Brągiel, A. Łukiewska, J. Rzącki, M. Nabiałek, Microstructure and some magnetic properties of bulk amorphous $(Fe_{0.61}Co_{0.10}Zr_{0.025}Hf_{0.025}Ti_{0.02}W_{0.02}B_{0.20})_{100-x}Y_x$ (x=0, 2, 3 or 4), Journal of Magnetism and Magnetic Materials 324 (2012) 540-549.

[8] R.A. Brand Improving the validity of hyperfine field distributions from magnetic alloys Nuclear Instruments and Methods in Physics Research B 28(1987) 398-416.

[9] P. Panissod, J. Durand, and J.I. Budnick, Nuclear Instruments and Methods in Physics 199/99 (1982) 27.

[10] A. Gupta, S.N. Kane, N. Bhagat, and T. Kulik, Journal of Magnetism and Magnetic Materials 254, 492 (2003).

[11] H. Kronmüller Micromagnetism in Amorphous Alloys IEEE Transactions on Magnetics 15 (1979) 1218-1225.

[12] H. Kronmüller Micromagnetism and Microstructure of Amorphous Alloys, Journal of Applied Physics. 52 (1981) 1859-1864.

[13] T. Holstein, H. Primakoff Field Dependence of the Intrinsic Domain Magnetization of a Ferromagnet Physical Review 58 (1940) 1098-1113.